Nano Energy 38 (2017) 101–108

Contents lists available at ScienceDirect

Nano Energy

journal homepage: www.elsevier.com/locate/nanoen

Full paper

High efficient harvesting of underwater ultrasonic wave energy by triboelectric nanogenerator

Yi Xi[b,c], Jie Wang[a,c], Yunlong Zi[c], Xiaogan Li[c], Changbao Han[a], Xia Cao[a], Chenguo Hu[b], Zhonglin Wang[a,c,d,*]

[a] Beijing Institute of Nanoenergy and Nanosystems Chinese Academy of Sciences Beijing, 100083 China
[b] Department of Applied Physics Chongqing University Chongqing, 400044 China
[c] School of Materials Science and Engineering Georgia Institute of Technology Atlanta, GA 30332-0245, USA
[d] CAS Center for Excellence in Nanoscience, National Center for Nanoscience and Technology (NCNST), Beijing 100190, China

ARTICLE INFO

Keywords:
TENG
Underwater energy
Ultrasonic wave
High efficient

ABSTRACT

Ultrasonic waves are existing in water and in our living environment, but harvesting the sonic wave energy especially in water is rather challenging, simply because of the high pressure generated by water. In this work, a triboelectric nanogenerator (TENG) has been designed using spherical pellets as the media for performing the contact-separation operation during ultrasonic wave excitation for energy harvesting. The fabricated TENG can attain an instantaneous output current from several milliamps to about one hundred milliamps and achieve an output power of 0.362 W/cm^2 at an ultrasonic wave frequency of 80 kHz. The average power conversion efficiency of the TENG has reached 13.1%. The equivalent output galvanostatic current is 1.43 mA, which is the highest value reported so far. The developed TENG pellets has been demonstrated to continuously power up to 12 lamps with 0.75 W each, and can continuously drive a temperature-humidity meter, an electronic watch, and directly drive a health monitor. This study presents the outstanding potential of TENG for underwater applications.

1. Introduction

Acoustic waves, which are rich in our living environment, are considered as a clean, sustainable and ubiquitous energy resource. Harvesting ultrasonic wave energy has been conducted through various mechanisms such as piezoelectric [1,2] and triboelectric [3–5] effects. Ocean is a rich source of acoustic waves, especially the ultrasonic waves, as generated naturally from animals and geological movements, and artificially from devices for underwater detection, communication, navigation and tracking [6,7]. Underwater ultrasonic energy harvesting especially that in deep ocean is extremely challenging due to the difficulties to effectively couple the acoustic waves with the energy harvesting device for energy conversion, as well as issues of durability and packaging. To date, the power outputs of currently reported underwater acoustic energy harvesters are rather low due to the low energy conversion efficiency [8].

To effectively harvest mechanical energy, our group has invented the nanogenerators in 2006 [9], which opens up a new era for energy harvesting and applications. Among them, triboelectric nanogenerator (TENG) invented in 2012 has drawn world-wide attention, due to its high output voltage and high output power [10–16]. Significant breakthroughs have been attained in harvesting acoustic energy by TENGs using organic film based and paper based structures and demonstrated especially useful at low frequency range (< 5 Hz) that are commonly emitted in daily life [4,5,17]. However, previous TENGs are still low in power output and energy conversion efficiency, especially that used underwater [18–21]. Moreover, these TENGs are not likely to be able to effectively harvest ultrasonic wave energy in the deep ocean environment owing to the pressure generated by water. New TENGs designed for effectively harvesting underwater ultrasonic wave energy are still highly demanded.

In this work, we report a high output current, high efficiency and low cost TENG for harvesting energy from ultrasonic wave under water. In comparison to traditional acoustic energy harvesting device, this device is more cost-effective, lighter in weight, and higher in efficiency, which make it ideal for harvesting ultrasonic energy underwater. A high output current of 0.12 A, and an energy average conversion efficient of 13.1% (The calculation method is presented in SI 1) have been achieved. So far [22,23], the equivalent output galvanostatic current achieves 1.43 mA, which is the highest value

* Corresponding author.
E-mail address: zlwang@binn.cas.cn (Z. Wang).

http://dx.doi.org/10.1016/j.nanoen.2017.04.053
Received 22 March 2017; Received in revised form 24 April 2017; Accepted 25 April 2017
Available online 24 May 2017

reported (5 cm × 5 cm × 1.27 cm in volume). The TENG (9 cm × 9 cm ×1.27 cm in volume) is demonstrated to power 12 lights in serial with the power of 0.75 W each. The TENGs are also proved to be a standard power source for various electronics including a temperature-humidity meter, an electronic watch and a health monitor. The proposed approach paves a paradigm-shift strategy to effectively utilize ultrasonic energy underwater and potentially collect acoustic signals in ocean.

2. Experimental

2.1. Fabrication of the TENG

The TENG consists of three parts. Properly designed cubic acrylic plates, being used to isolate and seal the pellets, were drilled the number of cylindrical holes. Two parallel Kapton film with Cu electrodes. Proper PTFE pellets were placed in the cylindrical hole. The cubic acrylic plates with cylindrical hole was assembled with the active dimensions of 5 cm × 5 cm × 1.27 cm and the other size including 9 cm × 9 cm × 1.27 cm for supporting electrodes. 25 μm thickness of the Kapton film was prepared, 500 nm thickness of the Cu film was coated on the prepared Kapton film, and coated Cu film of Kapton film was used to perform the top and bottom electrodes for device, respectively. The Cu electrode (5 cm × 5 cm × 0.01 cm) was fixed in parallel on the two outer surfaces of the acrylic plates as electrodes. PTFE pellets with the diameter of 1.6 mm, 2.38 mm and 3.3 mm were used to fill the cylindrical hole as negative materials and form the vibration units. Then the outside surface of the device was covered with thick water-proof to prevent the entrance of water.

2.2. Measurement and calculation of the device

The measurements were carried out at room temperature in underwater. The mechanical vibration of TENG was produced by the ultrasonic vibrator in the water. The vibration energy can be attained by the ultrasonic generator (UCE Ultrasonic (Group) Co., Ltd, China). The input power of ultrasonic wave has been attained by the ultrasonic power meter (Ultrasonic Equipment, YP0511A, China). The output voltage signal of TENG was acquired via a voltage preamplifier (Keithley 6514 System Electrometer) and the output current signal by a low-noise current preamplifier (Stanford Research System SR570). The potential distribution in the TENG was calculated from a finite-element simulation using Comsol Multiphysics software. During the electrical measurements, the serial and parallel circuit have been applied to avoid the preamplifier overflowed. The output current is the parallel circuit and the resistors are 100 Ω and 100 kΩ. The software platform is constructed based on LabVIEW, which can realize real-time data acquisition control and analysis. The output equivalent galvanostatic current was tested by the electrochemical workstation (Princeton Applied Research, Versa Stat3).

Due to the function of power conversion efficiency includes several important parameters, these parameters have to be defined. The maximum output power of TENG ($P_{out\ max}$) is defined as the formula (1),

$$P_{outmax} = V^2/R \quad (1)$$

where V is the output voltage with corresponding impedance matching (In the case of impedance matching, device in the best conditions, the maximum output power can be attained).

Then, the output power of TENG (P_{out}) is defined as the formula (2).

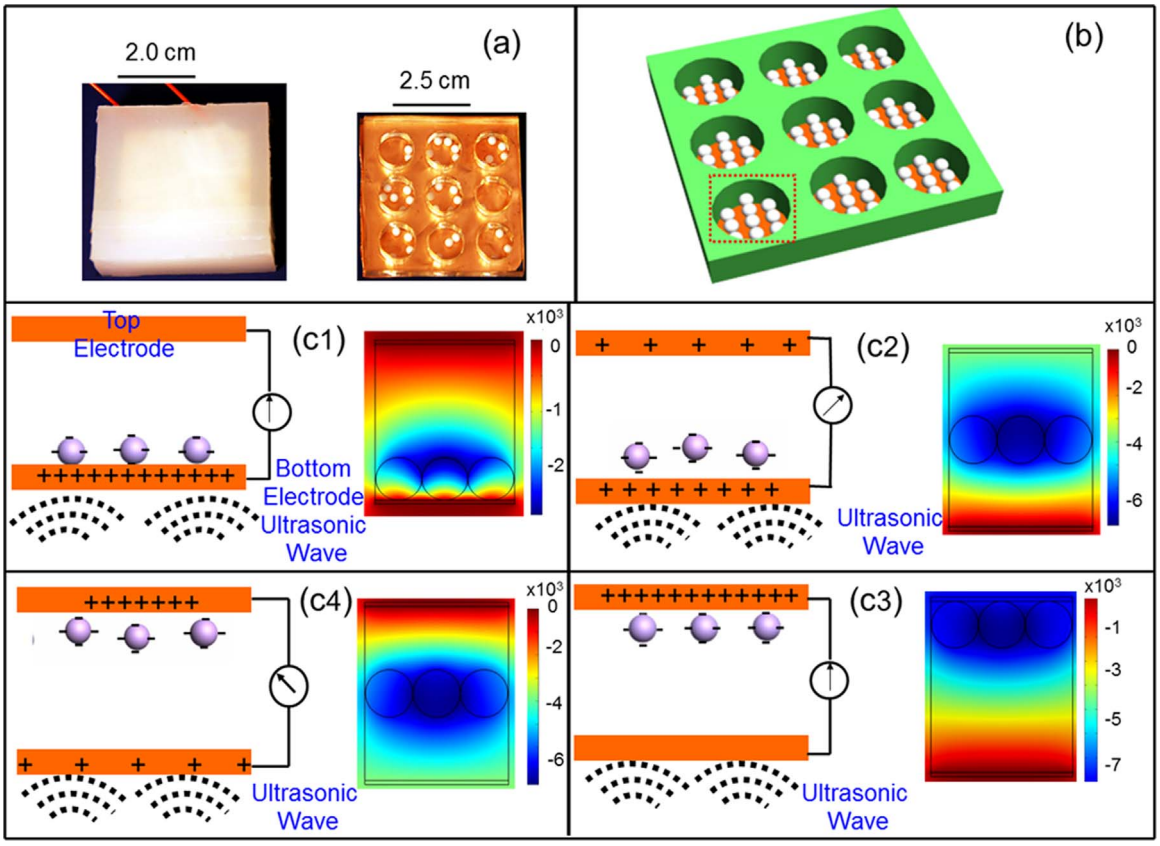

Fig. 1. Device design and working principle. (a) The photograph showing the packaged TENG and inter structure of TENG. (b)Three-dimensional structure schematic diagram of TENG. (c) Working principle of the device. (c1) Electrons injected process (left) and its potential distribution calculated by a finite-element simulation (right). (c2) The schematic diagram of triboelectric charge distribution and current generation process at the initial stage (left) and its potential distribution calculated by a finite-element simulation (right). (c3) The pellets collide with top electrode and move downward (left) and its potential distribution calculated by a finite-element simulation (right). (c4) PTFE balls move toward the bottom electrode and lead to current generation in reversed direction (left) and its potential distribution calculated by a finite-element simulation (right).

$$P_{out} = V^2/R \quad (2)$$

where V is the output voltage with the corresponding load resistance.

Finally, the corresponding formula of power conversion efficiency the is thus attained according to:

$$\eta = (P_{outmax}/P_{in}) \times 100\% \quad (3)$$

where P_{in} is the ultrasonic wave power ultrasonic, which is attained by testing with the ultrasonic power meter.

The effective electrode area is calculated by the two different methods. Firstly, based on the area of pellets, the effective area by calculated by the following formula.

$$S_{pellets} = n(\pi r^2)N \quad (4)$$

where n is the number of PTFE pellets in per cylindrical hole, r is the radius of PTFE pellet, N is the number of the cylindrical hole for cubic acrylic plates. Secondly, according to the structure of TENG, the effective area is the hole area for the device, the area of the holes (S_{holes}) for device including 7.065 cm^2 (9 and 25 holes) and 10.1736 cm^2 (16 holes).

Based on the number of pellets and the area of hole, the fill ratio (F) of device was attained, the details are as following. The pellets were used to fill the hole, based on the formula (4), the area of pellets in the holes can be calculated, and the area of hole is the same value in the effective area. The fill ratio can be calculated by the following formula,

$$F = S_{pellets}/S_{hole} \quad (5)$$

3. Results and discussion

3.1. Structural design and working principle of the TENG

As an energy harvesting device, the photograph of the TENG (9 holes, 5 cm × 5 cm × 1.27 cm) is shown in Fig. 1a. The TENG is mainly composed of PTFE pellets and two parallel Cu electrode plates fixed on an insulated cubic acrylic plate with the cylindrical hole, as shown in Fig. 1b (where the PTFE pellet has been found to be the best material for yielding out the output energy and these pellets are thus very light. Consequently, the increase in the weight of these pellets is almost negligible during power generation if the size doesn't increase too much (they cannot be changed too much since it's limited by the whole volume of the cube and the optimized number of pellets). Based on the triboelectric and electrostatic conduction effects, an alternating charge flow can be produced in an external load to form a sustainable power source [24]. The device works basically in accordance with the theoretical model of the freestanding type TENG as proposed in literature [25,26]. Two possible modes of motions such as the

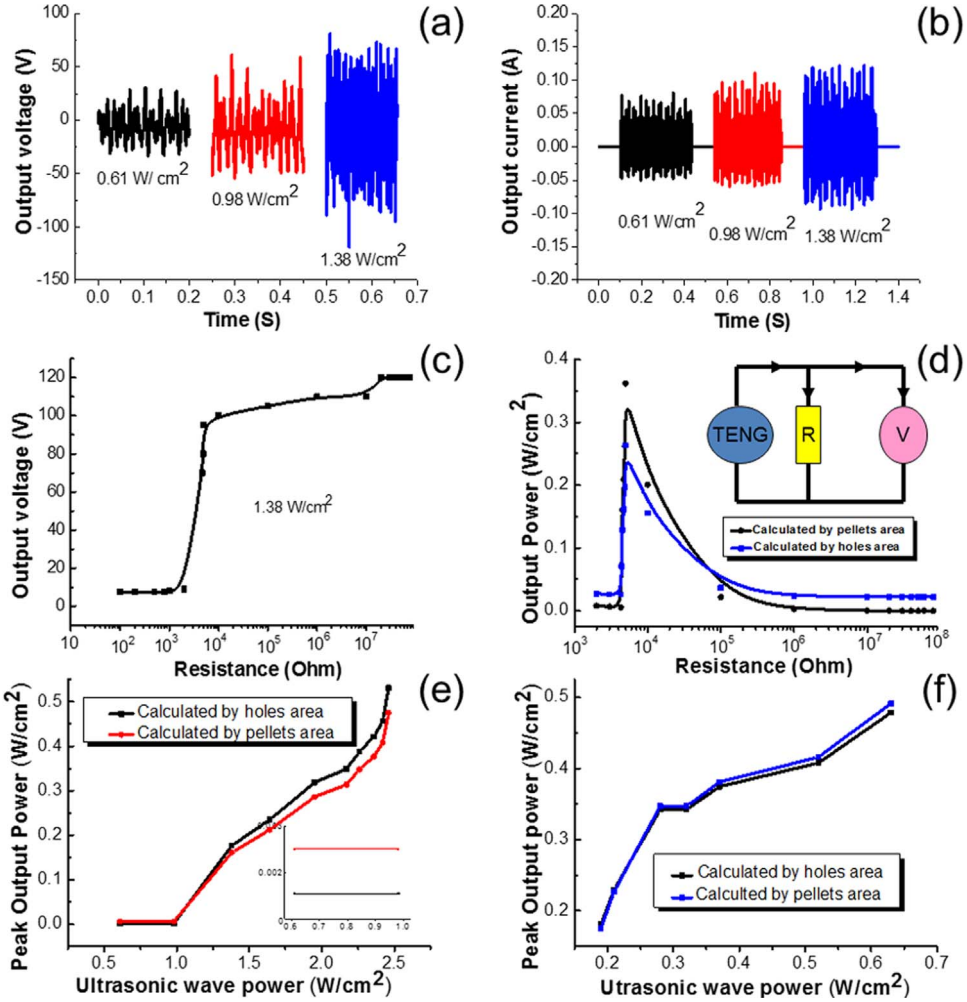

Fig. 2. (a–d) The output performance of the TENG for 9 holes and 7 pellets with 3.3 mm diameter (device 1) was driven by the ultrasonic wave power 0.61, 0.98 and 1.38 W/cm^2 at the frequency of 80 kHz. (a-b) The output voltage and the output current of TENG, respectively. (c-d) Dependence of the output voltage and the corresponding output power of the TENG on the external load resistances by the ultrasonic wave power 1.38 W/cm^2. The inset in (d) is the equivalent circuit diagram for (c-d). (c–d) The output power (Calculated by the pellets area and holes area) of device 1. (e–f) The output power (Calculated by the pellets area and holes area) for the 9 holes and the 12 pellets with 2.38 mm diameter (device 2) by the various ultrasonic wave powers at the frequency of 80 kHz (e) and 100 kHz (f), respectively. The ultrasonic wave power of 80 kHz: 0.61, 0.98, 1.38, 1.64, 1.95, 2.17, 2.26, 2.36 W/cm^2. The ultrasonic wave power of 100 kHz: 0.19, 0.21, 0.28, 0.32, 0.37, 0.52, 0.63 W/cm^2.

synchronous and asynchronous motions could participate in the collisions of the small pellets with the top and bottom electrodes under the activation of the applied ultrasonic vibration energy. Therefore, when the fabricated device is placed in underwater environment with the ultrasonic waves, the PTFE pellets on the cylindrical hole directly collide up and down between the two electrode plates as driven by the ultrasonic waves. When the pellets contact the bottom electrode, it would form the negative electrostatic charges on the surface of the PTFE pellets due to the high electron negativity of PTFE and the positive charges on the surface of the electrode, as electrons are injected from Cu electrodes into PTFE pellets due to triboelectrification effect (Fig. 1c1 left). The potential distribution within the small cube was calculated by using a finite-element simulation (right). It found the strong negative charges around the pellets and corresponding positive charges proximal to both surfaces of the electrodes. When the pellets move upward, the positive charges will flow from bottom electrode to the top electrode to achieve a new electrostatic balance, forming a current under short-circuit condition (Figure 1c2 left) [27]. Similarly, the potential distribution at this stage could also be well-predicted by using the finite-element simulation (right). After the pellets collide with top electrode and move downward (Fig. 1c3 left), according to its potential distribution calculated by the finite-element simulation (right), the positive charges in the top electrode will flow to the bottom electrode to return to the original electrostatic status. As a result, it would form a reverse current in the short-circuit condition as shown in Fig. 1c4 (left) as driven by the generated potential gradient calculated by the finite-element simulation (Fig. 1c4 right). This procedure forms the fundamental processes of converting ultrasonic wave energy into electricity. Based on the converting process, the generated current can essentially be described by the second terms (polarization charge) of the corresponding displacement current in the Maxwell equation as proposed by Wang [28].

$$\boldsymbol{J}_D = \frac{\partial \boldsymbol{D}}{\partial t} = \epsilon_0 \frac{\partial \boldsymbol{E}}{\partial t} + \frac{\partial \boldsymbol{P}}{\partial t} \tag{1′}$$

Thus, the corresponding displacement current density is expressed according to the equation:

$$J_D = \frac{\partial D_Z}{\partial t} = \frac{\partial \sigma_I(z,\,t)}{\partial t} = \sigma_c \frac{dz}{dt} \frac{d_1\epsilon_0/\epsilon_1 + d_2\epsilon_0/\epsilon_2}{[d_1\epsilon_0/\epsilon_1 + d_2\epsilon_0/\epsilon_2 + z]^2} \tag{2′}$$

where $\mathcal{E}_1$ and $\mathcal{E}_2$ are two dielectrics of permittivity, $\mathcal{E}_0$ is the vacuum of permittivity, d_1 and d_2 are the thickness of two dielectrics, σ_I(z, t) is the free electrons in the electrode, which is a function of the gap distance between two dielectrics. Clearly, the displacement current density is

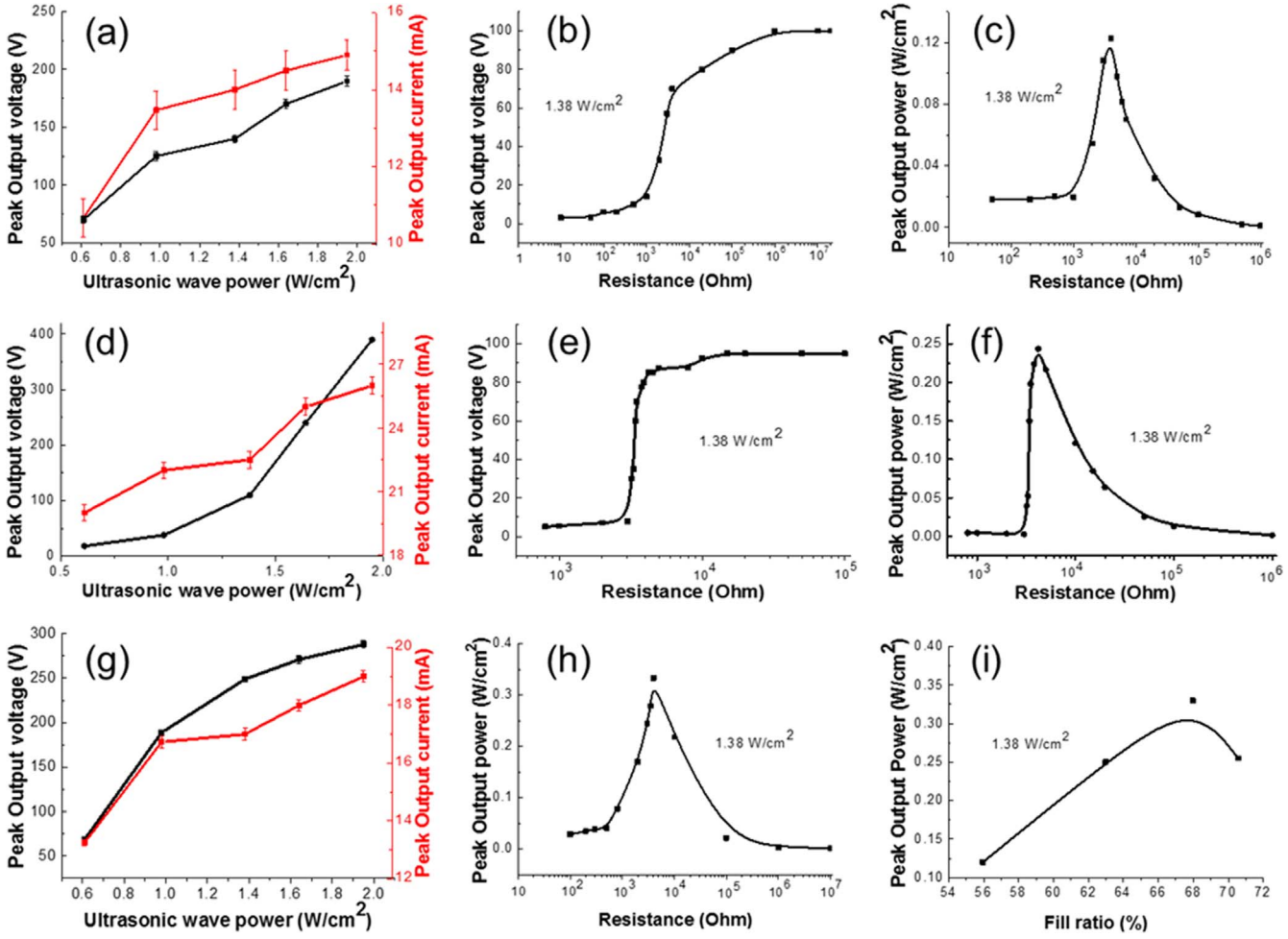

Fig. 3. The electrical output characterization of the optimized TENG as driven by ultrasonic wave at frequency of 80 kHz. (a–c) The electrical output of a TENG for 16 holes in the cubic acrylic plates with 1.27 cm thickness, and filled in 8 pellets per hole (device 3). (a) The output voltage and output current of device 3 under the different ultrasonic wave power with 80 kHz frequency. (b–c) The corresponding output voltage and output power of the device 3 on the different external load resistances. (d–f) The electrical output of TENG for the 25 holes and the 225 pellets with 1.6 mm diameter (device 4). (d) The output voltage and output current of device 4 under the different ultrasonic wave power with 80 kHz frequency. (e–f) The corresponding output voltage and output power of the device 4 on the different external load resistances. (g–h) The electrical output of a TENG for 9 holes in the cubic acrylic plates with 1.27 cm thickness, and filled in 12 pellets (2.38 mm diameter) per hole (device 2). (g) The output voltage and output current of device 2 under the different ultrasonic wave power. (h) The corresponding output power of the device 2 on the different external load resistances. (i) The different fill ratios and output power of four devices.

proportional to the charge density on the dielectric surface and the speed at which the two dielectrics are being separated or contacted. When the two dielectrics are driven to be in physical contact, electrostatic charges are transferred to the surfaces of the two owing to the contact electrification effect (triboelectricity), namely, the polarization charges density is higher, the electrostatic potential created by the polarization charges is balanced by the flow of electrons from one electrode to the other through an external load. This forms the basics of the output characteristics of the TENG [28]. Moreover, based on Maxwell's displacement current, when an external R was connected, the current transport equation is defined as [25]:

$$RA\frac{d\sigma_I(z,t)}{dt} = z\sigma_c/\epsilon_0 - \sigma_I(z,t)[d_1/\epsilon_1 + d_2/\epsilon_2 + z/\epsilon_0 \quad (3')$$

where z is a function of time t depending on the dynamic process that the force is applied.

3.2. Electrical Characterizations of the TENG

The electrical output performance of TENG with 9 holes on the cubic acrylic plate with 1.27 cm thickness, 7 pellets (diameter 3.3 mm) per hole (device 1) is demonstrated in Fig. 2(a-d). The fill ratio (F) of this TENG is 70.56%. The voltage and current outputs are illustrated with the ultrasonic wave frequency of about 80 kHz and ultrasonic wave power from 0.61 to 1.38 W/cm ^{2}. Fig. 2a shows the output voltages of device 1 and the peak voltage increased proportionally from ~60 V to ~170 V with the increasing ultrasonic wave power. Fig. 2b displays the output current of device 1 and it can reach 0.12 A at an ultrasonic wave power density of 1.38 W/cm ^{2}.

Fig. 2c shows the output voltage of device 1. It was found that the output voltage decreased as the loaded resistance increased. The corresponding output power is exhibited in Fig. 2d and the largest output power of device 1 can reach 0.362 W/cm^2 if taking the total surface area of the pellets as the effective area and 0.255 W/cm^2 if using the surface area of the holes as the effective area at the corresponding load resistance of 5 kΩ. Similarly, the effective conversion efficiency is 13.1% calculated using the total surface area of pellets and 9.3% if calculated using the surface area of holes (The detailed measurement and calculation methods are shown in measurement and calculation of the device). The entire device can be fully packaged and placed at even deep water because the current design can tolerate the pressure from water.

To further investigate the relationship between the output performance of TENG and the input performance of ultrasonic wave power, the output power of a TENG (The 9 holes on the cubic acrylic plate with 1.27 cm thickness, and filled in 12 pellets per hole with 2.38 mm diameter (device 2)) was demonstrated at different ultrasonic wave power and at frequency of 80 kHz and 100 kHz, and the results are shown in Fig. 2e and f. Fig. 2e displays the output powers at 80 kHz as a function of ultrasonic wave power, as calculated by the two different methods (refer to the measurement and calculation of device). The output powers always increase as the ultrasonic wave power increased, and the maximum output power about 0.55 W/cm ^{2} and 0.89 W/cm ^{2}, respectively. To further demonstrate the relationship between input power of ultrasonic wave and output power of the TENG, the different ultrasonic wave power at the frequency of 100 kHz was applied as shown in Fig. 2f. Using the same calculation method, it achieves the maximum output power of about 0.48 W/c m^2 and 0.62 W/cm ^{2}. It was found that the minimum power required to trigger the TENG at frequency of 80 kHz, shown in the insert of Fig. 2e, and then the output power of device 2 would increase as the input ultrasonic wave power increased. However, as driven by the ultrasonic wave at frequency of 100 kHz, the output power of device always improved as the input ultrasonic wave power increased. Furthermore, the output power at 80 kHz is smaller than that at 100 kHz. The results show the output signal is closely related to the input frequency and input power.

3.3. Structural optimization of the TENG

To attain a high efficient TENG, the different structural parameters of devices have been optimized including the hole number in the same area of cubic acrylic plate, the pellet size and fill ratio in the hole. Three devices have been fabricated to study the influence of pellet size and fill ratio on the output power characteristics of the TENG. The characterization of TENG electrical output has been exhibited in Fig. 3 with the different structure parameter. Fig. 3a-c show the electrical output of a TENG, which is 16 holes in the cubic acrylic plates with 1.27 cm thickness with each hole filled in 8 pellets (2.38 mm diameter) per hole (device 3). Fig. 3a demonstrates the output voltage and output current of device 3 varied with ultrasonic wave power from 0.61 to 1.95 W/cm ^{2} at the ultrasonic wave frequency of 80 kHz. As the ultrasonic wave power increased from the 0.61–1.95 W/cm ^{2}, the output voltage and current indicated a nonlinear augment up to the maximum of 180 V and 25 mA, respectively. Fig. 3b and c show the output voltages versus the load resistance and the corresponding output powers. The output power density of device 3 can reach 0.12 W/cm ^{2} under the load resistance of 4 kΩ. The plane fill ratio (F) of TENG is 55.95%, the detailed measurement and calculation methods are shown in measurement and calculation of the device. Fig. 3d-f exhibit the output performance of a TENG, which is 25 holes in the cubic acrylic plates with 1.27 cm thickness, and filled in 225 pellets with 1.6 mm diameter (9 pellets per hole) (device 4). The output voltage and output current of device 4 are also measured at the ultrasonic wave frequency of 80 kHz with the ultrasonic wave power varied from 0.61 to 1.95 W/cm ^{2} as shown in Fig. 3d. As the ultrasonic wave power increases, the output voltage and current were also found to increase to the maximum of 350 V and 23.5 mA, respectively. The enhanced output voltage compared to device 3 could be due to the fill ratio increased. Fig. 3e and f show the output voltages measured as the increase in the loaded resistance and the corresponding output powers. The largest output power density of this TENG is 0.25 W/cm ^{2} under a corresponding load resistance of 4.1 kΩ. The plane fill ratio (F) of TENG is 62.99%, the detailed measurement and calculation methods are shown in measurement and calculation of the device. Fig. 3g-h show the TENG, which has 9 holes on the cubic acrylic plate with 1.27 cm thickness, and filled with 12 pellets per hole and 2.38 mm in diameter (device 2). Fig. 3g clearly shows the output voltage and the output current of device 2 with the different ultrasonic wave power at a frequency of 80 kHz. The output voltage increases with increasing of the ultrasonic wave power, from 70 V to 288 V, meanwhile the current improve from 12 mA to 25 mA. Figure S1 exhibits the output voltages increase with the load resistance. Fig. 3h displays the output power at frequency of 80 kHz in the varied ultrasonic wave power, the results show the output powers are always increased as the ultrasonic wave power increased, and the maximum output power is about 0.33 W/cm ^{2}. The fill ratio of TENG is 67.97%, the detailed measurement and calculation methods are shown in measurement and calculation of the device. The different fill ratios and output power of four TENGs are displayed in Fig. 3i, the output power increases as the fill ratio increased when the fill ratio is below 67.97%, and then the output power will decrease as the fill ratio increased further. Hence, the realization of output power of TENG is related to the fill ratio of TENG, in agreement with previous theoretical report [27].

Since TENG is induced by the presence of the pellets, it is interesting to understand how it depends on the distribution of the pellets. We compare the results from a TENG structure without any pellets in the holes. And the corresponding output voltage and output current are displayed in Fig. S2 at frequency of 80 kHz and the input power 1.38 W/cm^2 of ultrasonic wave. From the data, we find that there is nearly no output voltage and current for the case of without any pellets of TENG, showing the pellets in our design play an important and crucial role.

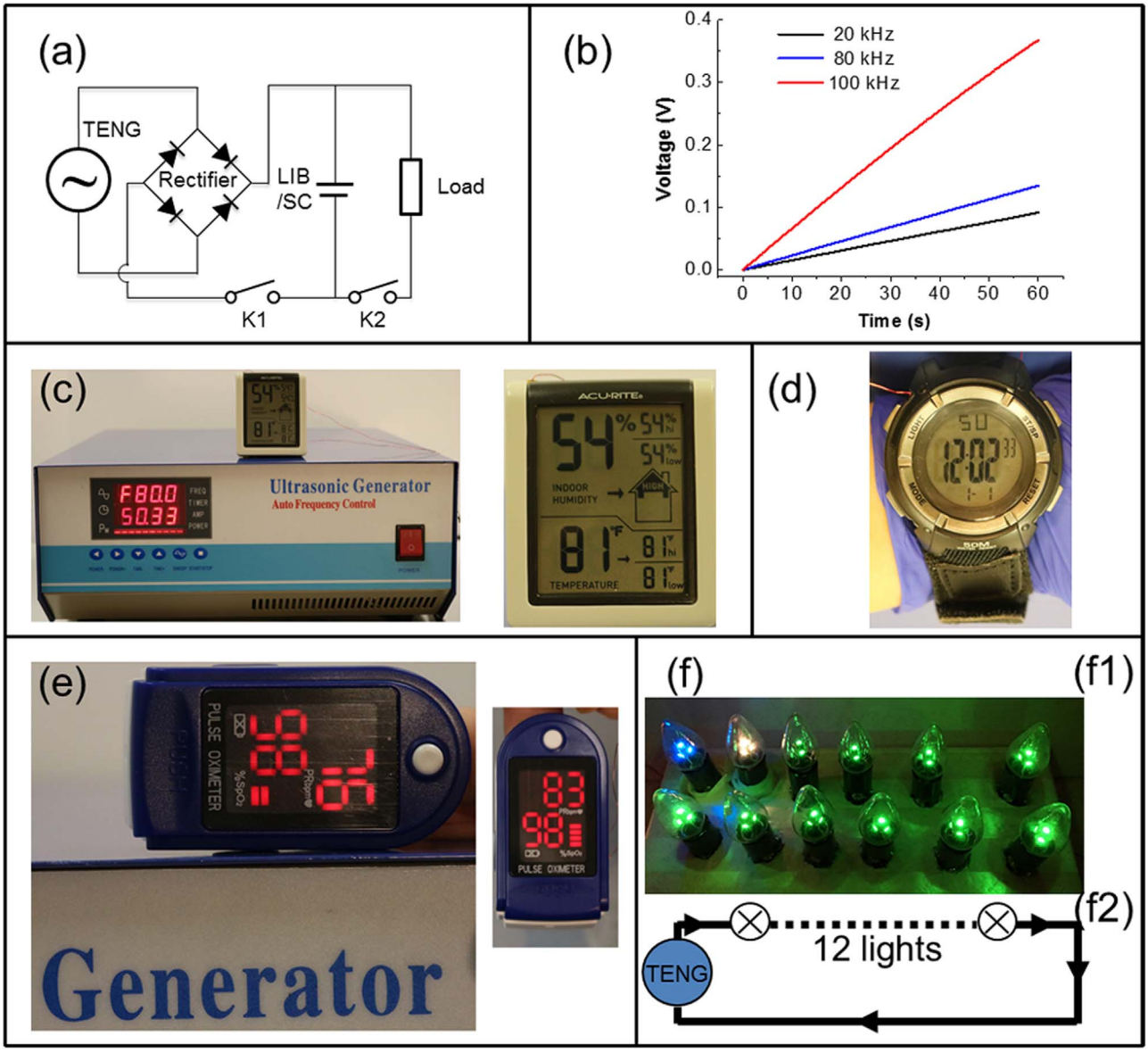

Fig. 4. Application of TENG for harvesting ultrasonic wave power under water. (a) Circuit diagram of TENG application. (b) Charging curves of the supercapacitor charged by the TENG at varied frequencies. (c) The photographs of the digital temperature–humidity (weather monitor) and (d) the electrical watch are continuously driven by TENG. (e) The photograph of the health monitor is directly driven by TENG. (f) The photograph of 12 lamps can be continuously lit by TENG, (f1) The photograph of 12 lit lamps with the TENG, (f2) The working equivalent circuit diagram for lamps.

3.4. Application of the TENG

To demonstrate the high output power and high conversation efficiency of TENG for harvesting ultrasonic wave energy under water as a sustainable and clean power source for practical application, the TENG has been demonstrated some real-scene applications as follows. Fig. 4a is the equivalent circuit of TENG for some practical applications. To further reveal its output equivalent galvanostatic current, the TENG (5 cm × 5 cm × 1.27 cm) was integrated with a supercapacitor (SC) to build a self-charging power system (SCPS) via a rectifier and the charging curves were tested. The charging rate is determined ascendant by the contacting frequency of device 1, as illustrated in Fig. 4b. The voltage of the supercapacitor increases by 91.4 mV during 60 s at frequency of 28 kHz, indicating an equivalent galvanostatic current of around 0.21 mA (The calculation method is presented in SI2). The voltage increases by 134.6 mV during 60 s of charging at frequency of 80 kHz, showing an equivalent galvanostatic current of about 0.45 mA. Furthermore, the supercapacitor is charged from 0 to 367 mV in 60 s at a frequency of 100 kHz, indicating an equivalent galvanostatic current of 1.43 mA, which is the maximum equivalent galvanostatic current reported for a TENG so far. The results demonstrate the equivalent galvanostatic current increased as the input ultrasonic wave frequency increased. Under ultrasonic wave at frequency of 80 kHz, the power delivered from TENG (5 cm × 5 cm × 1.27 cm) can serve as a power source to continuously drive a weather monitor and water-proof electrical watch which can be used in underwater (Fig. 4c and Supplement Video 1, Fig. 4d and Supplement Video 2). Furthermore, an enlarged TENG (9 cm × 9 cm × 1.27 cm) can supply even higher

output power. It can act as a power source to directly drive a health monitor (Fig. 4e and Supplement Video 3). It can also act as a power source to continuously and directly drive 12 lamps which can be employed as the navigation light (0.75 W per lamp) in serials, which is shown in Fig. 4f and Supplement Video 4, which demonstrate this TENG can be attained the output power about 7.5 W.

Supplementary material related to this article can be found online at doi:10.1016/j.nanoen.2017.04.053.

4. Conclusions

In summary, we have presented a novel high-efficiency TENG for harvesting ultrasonic wave energy underwater. The parameters of TENG have been optimized, and the output performance of TENG has been systematically characterized. The better output parameter is the structure parameter of 9 holes filled with 7 pellets with a diameter of 3.3 mm. Under input ultrasonic wave of 80 kHz and 1.38 W/cm ^{2}, the output peak voltage and current can attain about 170 V and 0.12 A, output power can be up to 0.362 W/cm ^{2}, and the power conversion efficiency can achieve 13.1%. The output equivalent galvanostatic current can achieve 1.43 mA, which is the largest one reported TENG. The device can continuously light 12 lamps with a power of 0.75 W per lamp, a temperature-humidity meter and an electronic watch, and directly drive a health monitor. The TENG presented here can be applied in shallow water and in deep water because the boxed structure can be fully packaged to tolerate the pressure from water. The TENG provides an effective, powerful, and simple solution for high-efficient energy harvesting of underwater ultrasonic energy.

Acknowledgements

Research was supported by the "thousands talents" program for pioneer researcher and his innovation team, China, the National Key R & D Project from Minister of Science and Technology (2016YFA0202704, 2016YFA0202702), National Natural Science Foundation of China (Grant No. 51432005, 5151101243, 51561145021), NSFCQ (cstc2014jcyjA50030) and the Chinese Scholars Council. The authors thank Tim Zhang and Dr. Ding for helpful discussion and continued support. Patents have been filed based on the research results presented in this manuscript.

Appendix A. Supporting information

Supplementary data associated with this article can be found in the online version at doi:10.1016/j.nanoen.2017.04.053.

References

[1] X.D. Wang, J.H. Song, J. Liu, Z.L. Wang, Science 316 (2007) 102–105.
[2] Q.F. Shi, T. Wang, T. Kobayashi, C. Lee, IEEE in: Proceedings of the 29th International Conference on Micro Electro Mechanical Systems (MEMS), 2016, pp. 1256–1259, 2016.
[3] J. Yang, J. Chen, Y. Liu, W.Q. Yang, Y.J. Su, Z.L. Wang, Acs Nano 8 (2014) 2649–2657.
[4] X. Fan, J. Chen, J. Yang, P. Bai, Z.L. Li, Z.L. Wang, Acs Nano 9 (2015) 4236–4243.
[5] A.F. Yu, M. Song, Y. Zhang, Y. Zhang, L.B. Chen, J.Y. Zhai, Z.L. Wang, Nano Res. 8 (2015) 765–773.
[6] D.A. Mann, D.M. Higgs, W.N. Tavolga, M.J. Souza, A.N. Popper, J. Acous. Soc. Am. 109 (2001) 3048–3054.
[7] M. Stojanovic, 2008, in: Proceedings of the Fifth Annual Conference on Wireless on Demand Network Systems and Services, 2008, DOI: Doi 10.1109/Wons.2008.4459349, pp. 1–10.
[8] S. Buogo, G.B. Cannelli, J. Acous. Soc. Am. 111 (2002) 2594–2600.
[9] Z.L. Wang, J.H. Song, Science 312 (2006) 242–246.
[10] F.R. Fan, Z.Q. Tian, Z.L. Wang, Nano Energy 1 (2012) 328–334.
[11] Y. Yang, H.L. Zhang, J. Chen, Q.S. Jing, Y.S. Zhou, X.N. Wen, Z.L. Wang, Acs Nano 7 (2013) 7342–7351.
[12] G. Zhu, Y.S. Zhou, P. Bai, X.S. Meng, Q.S. Jing, J. Chen, Z.L. Wang, Adv. Mater. 26 (2014) 3788–3796.
[13] H.Y. Guo, Q. Leng, X.M. He, M.J. Wang, J. Chen, C.G. Hu, Y. Xi, Adv. Energy Mater. 5 (2015) (1400790-1-5).
[14] F. Yi, X.F. Wang, S.M. Niu, S.M. Li, Y.J. Yin, K.R. Dai, G.J. Zhang, L. Lin, Z. Wen, H.Y. Guo, J. Wang, M.-H. Yeh, Y.L. Zi, Q.L. Liao, Z. You, Y. Zhang, Z.L. Wang, Sci. Adv. 2 (2016) (1501624-1-10).
[15] M.Y. Ma, Q.L. Liao, G.J. Zhang, Z. Zhang, Q.J. Liang, Y. Zhang, Adv. Funct. Mater. 25 (2015) 6489–6494.
[16] M.Y. Ma, Z. Zhang, Q.L. Liao, F. Yi, L.H. Han, G.J. Zhang, S. Liu, X.Q. Liao, Y. Zhang, Nano Energy 32 (2017) 389–396.
[17] J. Yang, J. Chen, Y.J. Su, Q.S. Jing, Z.L. Li, F. Yi, X.N. Wen, Z.N. Wang, Z.L. Wang, Adv. Mater. 27 (2015) 1316.
[18] X.F. Wang, S.M. Niu, Y.J. Yin, F. Yi, Z. You, Z.L. Wang, Adv. Energy Mater. 5 (2015) (1501467-1-9).
[19] G. Zhu, Y.J. Su, P. Bai, J. Chen, Q.S. Jing, W.Q. Yang, Z.L. Wang, Acs Nano 8 (2014) 6031–6037.
[20] J. Chen, J. Yang, Z. Li, X. Fan, Y. Zi, Q. Jing, H. Guo, Z. Wen, K.C. Pradel, S. Niu, Z.L. Wang, ACS Nano 9 (2015) 3324–3331.
[21] T. Jiang, L.M. Zhang, X.Y. Chen, C.B. Han, W. Tang, C. Zhang, L. Xu, Z.L. Wang, Acs Nano 9 (2015) 12562–12572.
[22] J. Wang, Z. Wen, Y.L. Zi, L. Lin, C.S. Wu, H.Y. Guo, Y. Xi, Y.L. Xu, Z.L. Wang, Adv. Funct. Mater. 26 (2016) 3542–3548.
[23] Y.L. Zi, S.M. Niu, J. Wang, Z. Wen, W. Tang, Z.L. Wang, Nat. Commun. 6 (2015) (8376-1-6).
[24] J. Chen, G. Zhu, W.Q. Yang, Q.S. Jing, P. Bai, Y. Yang, T.C. Hou, Z.L. Wang, Adv. Mater. 25 (2013) 6094–6099.
[25] S.M. Niu, Y. Liu, X.Y. Chen, S.H. Wang, Y.S. Zhou, L. Lin, Y.N. Xie, Z.L. Wang, Nano Energy 12 (2015) 760–774.
[26] S.M. Niu, Z.L. Wang, Nano Energy 14 (2015) 161–192.
[27] C.B. Han, T. Jiang, C. Zhang, X.H. Li, C.Y. Zhang, X. Cao, Z.L. Wang, Acs Nano 9 (2015) 12552–12561.
[28] Z.L. Wang, Mater Today, http://dx.doi.org/10.1016/j.mattod.2016.12.001.

Yi Xi received her Ph.D. in 2010 in Physics from Chongqing University, China. Now she is an associate professor at Chongqing University, China. Her main research interests focus on the fields of piezoelectric, triboelectric nanogenerators for energy harvesting and supercapacitors for energy storage, driving some personal electronic devices.

Dr. Jie Wang is currently a professor at Beijing Institute of Nanoenergy and Nanosystems, Chinese Academy of Sciences. His main research interests focus on the energy materials, self-powered system, supercapacitors and nanogenerators.

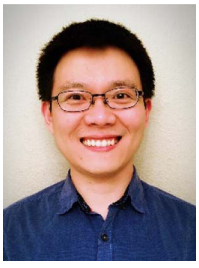

Dr. Yunlong Zi received his Bachelor of Engineering from Department of Materials Science and Engineering at Tsinghua University, Beijing, China, in 2009, and his PhD from Department of Physics at Purdue University, West Lafayette, Indiana, USA, in 2014. He is currently working as a postdoctoral fellow at Georgia Institute of Technology under supervision of Prof. Zhong Lin Wang. His research interests include fundamental physics of triboelectric nanogenerators, hybrid nanogenerator for energy harvesting, self-powered systems, nanoelectronics and synthesis of semiconductor nanomaterials. As the 1st authors, his research have been published in top journals, including Nature Nanotechnology, Nature Communications, Advanced Materials, Nano Letters and etc. He was honored as the winner of MRS Postdoctoral Award by Materials Research Society in 2017, as the first recipient from Georgia Tech; and one of "5 students who are transformation makers" by Purdue University in 2013, as highlighted in Purdue homepage.

Xiaogan Li is an associate professor in the School of Microelectronics in Dalian University of Technology, Dalian, Liaoning, P.R. China. He received his Ph.D. in Materials Science and Engineering from University of Leeds, U.K. and conducted two-year postdoctoral research in chemical gas sensors at The Ohio State University in USA. His current research interests are in chemical gas sensors and electrochemical energy devices.

Dr. Chang Bao Han received his Ph. D degree from Zhengzhou University in 2012. He firstly fabricated self-powered triboelectric filter to realize the effective removal of PMs in automobile exhaust without applying an external power. His work opens up an entirely new approach of cleaning PMs by a self-powered triboelectric device.

Prof. Xia Cao is currently a distinguished professor at University of Science and Technology Beijing, and a professor at Beijing Institute of Nanoenergy and Nanosystems, Chinese Academy of Sciences. Her main research interests focus on the energy materials, nanoelectroanalytical chemistry, self-powered nano-biosensors and piezoelectric sensors.

Chenguo Hu is a professor of physics in Chongqing University and the director of Key Lab of Materials Physics of Chongqing Municipality. She received her Ph.D. in Materials from Chongqing University in 2003. Her research interests include methodology of synthesizing functional nanomaterials, investigation of morphology and size dependent physical and chemical properties of nanomaterials, and design and fabrication of electronic devices, such as nanogenerators and sensors.

Zhong Lin (ZL) Wang received his Ph.D. from Arizona State University in physics. He now is the Hightower Chair in Materials Science and Engineering, Regents' Professor, Engineering Distinguished Professor and Director, Center for Nanostructure Characterization, at Georgia Tech. Dr. Wang has made original and innovative contributions to the synthesis, discovery, characterization and understanding of fundamental physical properties of oxide nanobelts and nanowires, as well as applications of nanowires in energy sciences, electronics, optoelectronics and biological science. His discovery and breakthroughs in developing nanogenerators established the principle and technological road map for harvesting mechanical energy from environment and biological systems for powering personal electronics. His research on self-powered nanosystems has inspired the worldwide effort in academia and industry for studying energy for micro-nano-systems, which is now a distinct disciplinary in energy research and future sensor networks. He coined and pioneered the field of piezotronics and piezo-phototronics by introducing piezoelectric potential gated charge transport process in fabricating new electronic and optoelectronic devices. Details can be found at: http://www. nanoscience.gatech.edu.